J. Phys. Chem. A **2009,** *113,* 11075–11083

Reactions of Ionized Methyl Benzoate with Methyl Isocyanide in the Gas Phase: Nucleophilic Aromatic Substitutions vs Hydrogen Migrations

Guy Bouchoux*

Laboratoire des Mécanismes Réactionnels, UMR CNRS 7651, Département de Chimie, Ecole Polytechnique, Palaiseau Cedex, France

Robert Flammang, Julien De Winter, and Pascal Gerbaux*

Laboratory of Organic Chemistry—Center of Mass Spectrometry, University of Mons, Place du Parc 20, B-7000 Mons, Belgium

Received: July 22, 2009; Revised Manuscript Received: August 27, 2009

The chemistry leading to the competitive eliminations of H, CH_3, and $OCOCH_3$ from adducts of ionized methyl benzoate and neutral methyl isocyanide has been explored using density functional theory molecular orbital calculations. The energies of the various reactants and transition structures were estimated at the B3LYP/6-31+G(d,p) level of theory. Nucleophilic aromatic substitution is proposed to account for the H and $OCOCH_3$ eliminations. The corresponding σ-complex intermediates, $\mathbf{B_{1ipso}}$ and $\mathbf{B_{1ortho}}$, are stable species lying in deep energy wells situated 70 and 120 kJ/mol, respectively, below the reactants, ionized methyl benzoate and methyl isocyanide. The latter complex, $\mathbf{B_{1ortho}}$, may be also at the origin of a multistep rearrangement involving hydrogen migrations and methyl elimination from the original methoxy group of the benzoate moiety.

Introduction

Nucleophilic aromatic substitution is a major class of chemical reaction, extensively used in synthetic organic chemistry.[1,2] Since the Wheland proposal,[3] this kind of reaction is generally assumed to follow an addition–elimination process involving the passage through a (stable or transient) σ-complex intermediate. Nucleophilic aromatic substitution is expected to easily occur if the nucleophile reacts with an electron deficient aromatic compound. The more usual way consists of using electron-withdrawing substituents to activate the aromatic substrate. A second possibility is to ionize the aromatic molecule, for example, by electron removal. If, in the former case, anionic nucleophiles are necessary for the reaction to occur, the latter situation allows the use of neutral nucleophiles. In both cases, the knowledge of the intrinsic mechanism of the aromatic substitution may be amply favored by gas phase studies of isolated species, without the presence of solvent molecules or counterions. Accordingly, recent gas phase experiments, where detection of the reaction intermediate is done after photoionization of neutral 1:1 clusters and characterization of the resulting ionized adduct by its photodissociation IR spectrum, demonstrate the occurrence of stable σ-complex intermediates in both anionic[4] and cationic gas phase nucleophilic aromatic substitution.[5,6]

Compared to the wealth of information on anionic nucleophilic aromatic substitution in solution[1,2] and in the gas phase,[4,7] reactions involving positively charged aromatic substrates are less documented. Concerning such gas phase cationic nucleophilic aromatic substitution, former studies were essentially devoted to reactions between ionized halobenzene and ammonia either into photoionized van der Waals complexes[8−11] or by a bimolecular process in a Fourier transform ion cyclotron resonance (FT-ICR) mass spectrometer.[12−14] It was concluded from these studies that chloro-, bromo-, and iodobenzene radical cations react with ammonia in an ipso substitution to yield anilinium ions. The generally low efficiency of the reaction and the fact that iodobenzene reacts more slowly, in spite of a lower dissociation energy of the C−I bond, has been interpreted by an addition−elimination process where the first step is rate determining. Beside these thorough but limited studies, a need for the finding of other examples of cationic nucleophilic aromatic substitution reactions is consequently evident in order to have a more general picture of this type of reaction and to provide new insight into its mechanism. In this context, we have recently shown that, in the gas phase, methyl isocyanide, CH_3NC, is an efficient nucleophilic reagent.[15−18] This is the result of its high ionization energy (11.24 eV) and its relatively low proton affinity (839 kJ/mol)[19] which prevents charge and proton exchange processes. Moreover, the high dipole moment of CH_3NC (3.85 D) favors its association with charged species and consequently increases its reaction efficiency. During these previous investigations, we observed that ionized methyl benzoate reacts readily with neutral methyl isocyanide in the hexapole collision cell of a six-sector mass spectrometer.[17,18] The observed product ions *m/z* 176, 162, and 118 formally correspond to elimination of a hydrogen atom, a methyl radical, and a $C_2H_3O_2$ radical, respectively, from the ionized methyl benzoate and methyl isocyanide adduct (*m/z* 177). The major product ion, *m/z* 118, corresponds to the elimination of the original methoxycarbonyl group, and its structure has been established to be *N*-methylated benzonitrile, $CH_3N^+{\equiv}C{-}C_6H_5$.[18] These data strongly suggest that the *m/z* 118 ion results from a nucleophilic aromatic substitution. Furthermore, the competitive formation of *m/z* 176 ions may be also interpreted by an aromatic substitution mechanism. Finally, it has been observed that the reaction leading to *m/z* 162 ions involves exclusively the loss of the methyl group of the $COOCH_3$ moiety.[18] This is quite surprising since it is known that direct methyl loss from ionized methyl carboxylates is a very energy-demanding process. The reaction channel resulting in the methyl loss is consequently a

10.1021/jp906942e CCC: $40.75

complicated process, probably involving rearrangement reactions. From this point of view, it may be noted that ionized methyl benzoate itself is prone to significant rearrangement processes.[20−22]

The goal of the present study is to explore in detail the chemistry leading to the eliminations of H, CH_3, and $OCOCH_3$ after ion/molecule reaction between ionized methyl benzoate and neutral methyl isocyanide. For this purpose, the nucleophilic aromatic substitution pathways leading to H and $OCOCH_3$ eliminations and several reaction paths allowing an explanation of the CH_3 loss were examined by means of density functional theory molecular orbital calculations at the B3LYP/6-31+G(d,p) level.

Calculations

Quantum chemical calculations were carried out using the Gaussian 03 set of programs[23] within the frame of the density functional theory. Geometry optimizations of the stationary points and the corresponding transition structures connecting the relevant equilibrium structures were conducted at the B3LYP/6-31+G(d,p) level of theory. Vibrational frequencies were calculated at this level using the harmonic oscillator approximation. The identity of local minima and transition structures were determined by the absence or presence of only one negative value, respectively. Second, unscaled B3LYP/6-31+G(d,p) frequencies were used to compute zero-point vibrational energies and vibrational contributions to 298 K enthalpies. Several reviews were recently devoted to the evaluation of the various performances of density functional methods.[24−30] In particular, the ability of the B3LYP hybrid functional combined with Pople-type polarized basis sets to reproduce relative energies of conformers[24−27] or bond dissociation and radical stabilization energies[28−30] is well documented. From these overviews, it appears that the error associated with enthalpies computed at these levels rarely exceeds 5−10 $kJ \cdot mol^{-1}$. This energy range may provide an estimate of the accuracy expected on the present data.

The computational results are summarized in Table 1. All energetic data are given in hartree (total energies and enthalpies) or in $kJ \cdot mol^{-1}$ (relative energies and enthalpies, 1 hartree = 2625.5 kJ mol^{-1}).

Results and Discussion

As recalled from the Introduction, the most abundant ionic product resulting from the reaction between ionized methyl benzoate and neutral methyl isocyanide appears at *m/z* 118 (100%). It originates from loss of the original methoxycarbonyl group as revealed by deuterium labeling.[17,18] Furthermore, the structure of the *m/z* 118 ion has been established to be $CH_3N^+{\equiv}C{-}C_6H_5$ ions by comparison of its collisional activation spectrum (see Figure 3a in ref 16) with that of *N*-methylated benzonitrile.[18] Two less important signals are observed at *m/z* 162 (∼10%) and *m/z* 176 (∼2%). They correspond to the eliminations of a methyl radical and a hydrogen atom, respectively, from a 1:1 complex (*m/z* 177) between ionized methyl benzoate (*m/z* 136) and methyl isocyanide (MW 41). Using isotopologues of methyl benzoate, namely, methyl benzoate-d_5 (ring deuterated) and methyl benzoate-d_3 (methyl deuterated), it was shown that the hydrogen atom lost arises specifically from the benzene ring while the methyl and methoxycarbonyl losses imply exclusively the ester function.[17,18]

Reaction between ionized methyl benzoate, **A** (which is more stable in its syn conformation, Table 1), and methyl isocyanide may lead to several type of adducts: (i) ion−neutral complexes, characterized by a long distance between the two closest atoms pertaining to each reactant, and (ii) covalently bound species (i.e., σ-complexes). The five structures resulting from the formation of a covalent bond between the sp-hybridized carbon of methyl isocyanide and various receptor sites of ionized methyl benzoate are presented in Scheme 1.

The four covalent structures $\mathbf{B_{1ortho}}$, $\mathbf{B_{1meta}}$, $\mathbf{B_{1para}}$, and $\mathbf{B_{1ipso}}$, originating from the addition of methyl isocyanide on the phenyl ring, are significantly stabilized with respect to the separated reactants **A** + CH_3NC. The relative enthalpies at 298 K calculated at the B3LYP/6-31+G(d,p) level are indicated below each structure in Scheme 1 (in kJ mol^{-1}, see also Table 1). Interestingly enough, the radical character of these four radical cations is essentially located on the benzenic part, while the positive charge is shared between the two substituents. Mulliken population analysis shows that the spin density is distributed among the three carbon atoms situated in ortho and para position with respect to the sp^3 carbon of the ring. It is also worthy to note that the $\mathbf{B_{1ortho}}$ structure is by far the most stable since it is situated 120 kJ mol^{-1} below **A** + CH_3NC whereas the three other structures are in the 70−94 kJ mol^{-1} range (Table 1 and Scheme 1). This situation is probably due to a favorable interaction between the oxygen of the carbonyl group and the nitrilium moiety.

The fifth structure, $\mathbf{B_{1oxo}}$, results from the addition of the methyl isocyanide to the oxygen of the carbonyl group. This structure is the least stable, as it lies only 38 kJ mol^{-1} below **A** + CH_3NC. Mulliken population analysis indicates that in $\mathbf{B_{1oxo}}$ the positive charge is concentrated on the carbon of the carboxyl group while the unpaired electron is located on the nitrogen atom.

From these five primary structures, $\mathbf{B_{1xxx}}$, various processes may be envisaged in order to explain the dissociation reactions leading to *m/z* 118 ($OCOCH_3$ loss), 162 (CH_3 loss), and 176 (H loss) ions. We investigated a number of pathways involving simple bond elongations but also more complex rearrangements including hydrogen migrations or cyclization reactions. A survey of this extensive exploration will be depicted below.

Methoxyacylium Radical ($OCOCH_3$) Loss. This constitutes the major reaction route. The structure of the product ion, *m/z* 118, has been clearly established to be *N*-methylated benzonitrile, **G**, from collisional activation experiments.[18] Accordingly, significant signals are observed at *m/z* 77 and 51 in the CA spectrum of *m/z* 118 ions, thus pointing to a monosubstituted benzenic structure. The series *m/z* 103, 76, and 50, also observed in the same CA spectrum, is in agreement with an initial methyl loss leading to ionized benzonitrile and its subsequent dissociation products. This assignment is further corroborated by the fact that this CA spectrum is identical to that obtained after methylation of benzonitrile itself by chloromethane in a chemical ionization source. Finally, other structures, such as protonated toluidine or benzyl cyanide and methylated phenyl isonitrile, were excluded on the basis of their very different CA spectra.

As indicated in the Introduction, formation of ion **G** from reaction between ionized methyl benzoate, **A**, and methyl isocyanide is a priori possible by an addition−elimination process involving intermediate structure $\mathbf{B_{1ipso}}$. From a thermodynamic point of view, the products **G** + $^{\bullet}OCOCH_3$ are predicted to be situated 71 kJ mol^{-1} below **A** + CH_3NC (B3LYP/6-31+G(d,p) computed ΔH°_{298} value, Table 1; experimental value is −96 kJ mol^{-1}[31]). The overall reaction is consequently allowed to occur if no critical energy barrier separates reactants and products. In order to test this hypothesis, we explore the energy profile associated with the overall process

TABLE 1: Total (hartree) and Relative[a] (kJ mol^{-1}) Energies Calculated at the B3LYP/6-31+G(d,p) Level

structure	E_0°	H_0°	H_{298}°
A (syn)	−459.826846	−459.685480	−459.675180
A (anti)	−459.814083	−459.672519	−459.662092
G: $CH_3NCC_6H_5^+$	−364.171580	−364.032646	−364.023231(−149)
CH_3NC	−132.730165	−132.684910	−132.680179
H•	−0.500273	−0.500273	−0.497914
CH_3•	−39.847335	−39.817522	−39.813527
CO_2	−188.590393	−188.578828	−188.575246
$OCOCH_3$	−228.413832	−228.364902	−228.359142
A + CH_3NC	−592.557011(0)	−592.370390(0)	−592.355359(0)
G + $OCOCH_3$	−592.585412	−592.39754(−71)	−592.382373(−71)
$\mathbf{B}_{\mathbf{1ortho}}$	−592.606083	−592.415366	−592.401021(−120)
$\mathbf{B}_{\mathbf{1meta}}$	−592.592021	−592.401967	−592.387441(−84)
$\mathbf{B}_{\mathbf{1para}}$	−592.595927	−592.405491	−592.391045(−94)
$\mathbf{B}_{\mathbf{1ipso}}$	−592.586261	−592.396770	−592.381936(−70)
$\mathbf{B}_{\mathbf{1oxo}}$	−592.575509	−592.384018	−592.369777(−38)
$\mathbf{B}_{\mathbf{1oxo'}}$	−592.583258	−592.394389	−592.377819(−59)
$\mathbf{B}_{\mathbf{3ortho}}$	−592.623488	−592.432782	−592.418222(−165)
$\mathbf{B}_{\mathbf{2ortho}}$	−592.616980	−592.426081	−592.411572(−148)
$\mathbf{C}_{\mathbf{1ortho}}$	−592.616341	−592.424616	−592.410200(−144)
$\mathbf{C}_{\mathbf{1ortho'}}$	−592.621293	−592.430161	−592.415170(−157)
$\mathbf{C}_{\mathbf{1ortho''}}$	−592.617871	−592.426869	−592.412835(−151)
$\mathbf{C}_{\mathbf{1ortho'''}}$	−592.618578	−592.427653	−592.413570(−153)
$\mathbf{C}_{\mathbf{1ortho''''}}$	−592.616838	−592.425261	−592.410603(−145)
$\mathbf{C}_{\mathbf{2ortho}}$	−592.624412	−592.434035	−592.420214(−170)
$\mathbf{C}_{\mathbf{2ortho'}}$	−592.630790	−592.438269	−592.424743(−182)
$\mathbf{D}_{\mathbf{1}}$	−592.576404	−592.387906	−592.372897(−46)
$\mathbf{D}_{\mathbf{2}}$	−592.598386	−592.409400	−592.393232(−99)
$\mathbf{D}_{\mathbf{3}}$	−592.579099	−592.390007	−592.374334(−50)
TSB1/C2	−592.556534	−592.371342	−592.357326(−5)
TSB1/C1	−592.567106	−592.380683	−592.366623(−30)
TSC1/C2	−592.611385	−592.420570	−592.407078(−136)
TSB1/B3	−592.551617	−592.365689	−592.351146(+11)
TSB1/B2	−592.551077	−592.364807	−592.350331(+13)
TSB1/E1	−592.555967	−592.373554	−592.358152(−7)
TSB1/D1	−592.571018	−592.382208	−592.367514(−37)
TSB1/D2	−592.568140	−592.380125	−592.365249(−26)
$\mathbf{E}_{\mathbf{1ortho}}$	−592.065505	−591.883776	−591.869928(−33)
$\mathbf{E}_{\mathbf{1ortho'}}$	−592.056670	−591.875148	−591.861175(−10)
$\mathbf{E}_{\mathbf{1ortho''}}$	−592.042339	−592.860854	−591.847041(+27)
$\mathbf{E}_{\mathbf{2ortho}}$	−592.058205	−591.875350	−591.862625(−14)
$\mathbf{E}_{\mathbf{2ortho'}}$	−592.052083	−591.869122	−591.856321(+3)
$\mathbf{E}_{\mathbf{2ortho''}}$	−592.049731	−591.866384	−591.853936(+9)
$\mathbf{E}_{\mathbf{2ortho'''}}$	−592.041340	−591.858144	−591.845541(+31)
$\mathbf{E}_{\mathbf{1meta}}$	−592.059107	−591.877615	−591.864529(−19)
$\mathbf{E}_{\mathbf{1para}}$	−592.057248	−591.875783	−591.861774(−11)
$\mathbf{F}_{\mathbf{phta}}$	−552.745311	−552.590631	−552.579603(−99)
$\mathbf{F}_{\mathbf{phta''}}$	−552.739593	−552.584768	−552.573853(−84)
$\mathbf{F}_{\mathbf{phta'}}$	−552.738648	−552.583648	−552.572690(−81)
$\mathbf{F}_{\mathbf{phta'''}}$	−552.731505	−552.576631	−552.565648(−63)
$\mathbf{F}_{\mathbf{oxazo}}$	−552.713259	−552.557521	−552.547018(−14)
$\mathbf{F}_{\mathbf{carboxo}}$	−552.726565	−552.575967	−552.561731(−52)
$\mathbf{F}_{\mathbf{C1ortho'}}$	−552.742928	−552.589780	−552.577511(−94)
$\mathbf{F}_{\mathbf{C1ortho'}}$	−552.749371	−552.595744	−552.583568(−110)
$\mathbf{F}_{\mathbf{C1ortho}}$	−552.757141	−552.603243	−552.591180(−129)

[a] Relative 298 K enthalpies indicated in parentheses in the last column are energies of the fragmentation products, or reaction intermediates, evaluated with respect to the separated reactants **A** + CH_3NC.

SCHEME 1

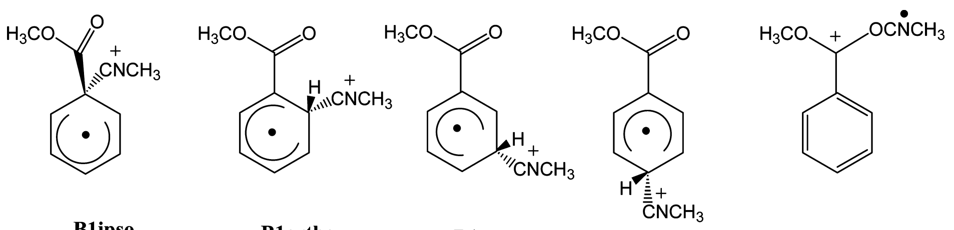

B1ipso -70

B1ortho -120

B1meta -84

B1para -94

B1oxo -38

SCHEME 2

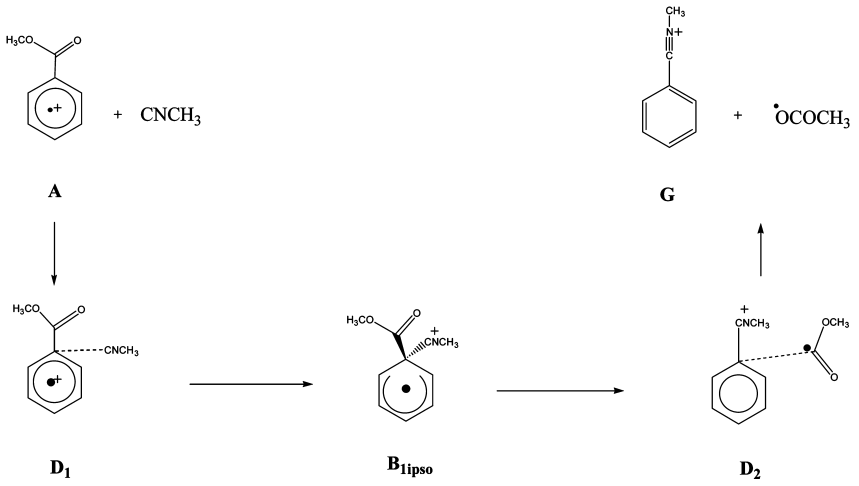

A + CH$_3$NC → **G** + $^{\bullet}$OCOCH$_3$. The results of this investigation are summarized in Scheme 2 and Figure 1.

As described in Scheme 2, this nucleophilic aromatic substitution reaction follows a multistep path involving two ion−neutral complexes (**D1** and **D2**) and the covalently bound intermediate $\mathbf{B_{1ipso}}$. The first approach complex **D1** consists of an ion−neutral complex between ionized methyl benzoate and neutral methyl isocyanide which, at the B3LYP/6-31+G(d,p) level, is situated 46 kJ mol^{-1} below the reactants (298 K enthalpy). The distance separating the two components of the complex, C(1).. .CNCH$_3$, is equal to 2.60 Å. Starting from **D1**, formation of the covalent complex $\mathbf{B_{1ipso}}$ formally involves breaking the aromaticity of the benzene ring during the formation of the new C(1)−C NCH$_3$ bond. A modest, but sizable, critical energy (of 14 kJ mol^{-1}) is associated with this step indicating a clear balance between the aromaticity breaking and the C−C bond formation. The critical structure **TSB1/D1** presents a C.. .C distance equal to 1.90 Å; its shortening to 1.45 Å in structure $\mathbf{B_{1ipso}}$ is accompanied by a stabilization of 38 kJ mol^{-1}.

The formation of the products **G** + $^{\bullet}$OCOCH$_3$ has been studied by elongating the C(1)−COOCH$_3$ bond from $\mathbf{B_{1ipso}}$. As observed for the **D1** → $\mathbf{B_{1ipso}}$ step, this reaction is accompanied by an increase of potential energy since the complete C(1)−COOCH$_3$ bond elongation is necessary to recover the full aromaticity of the ring. Accordingly, starting from $\mathbf{B_{1ipso}}$, the total energy of the system increases significantly before attaining a maximum and then decreases while the CNCH$_3$ moiety and the benzene ring approach planarity. The corresponding transition structure, **TSB1/D2**, has been located. It is characterized by a C−C distance of 2.09 Å and a 298 K enthalpy equal to 44 kJ mol^{-1} with respect to $\mathbf{B_{1ipso}}$. An ion−neutral complex between methylated benzonitrile and the $^{\bullet}$OCOCH$_3$ radical has been located. This structure, **D2**, lies 99 kJ mol^{-1} below **A** + CH$_3$NC and 28 kJ mol^{-1} below **G** + $^{\bullet}$OCOCH$_{3.}$ As evident from examination of Figure 1, all these processes occur below the energy level of the reactants, and the overall aromatic substitution reaction summarized in Scheme 2 is thermodynamically allowed. We note that the rate-determining step is the $\mathbf{B_{1ipso}}$ → **D2** process, and the corresponding transition structure, **TSB1/D2**, is situated 26 kJ mol^{-1} below **A** + CH$_3$NC.

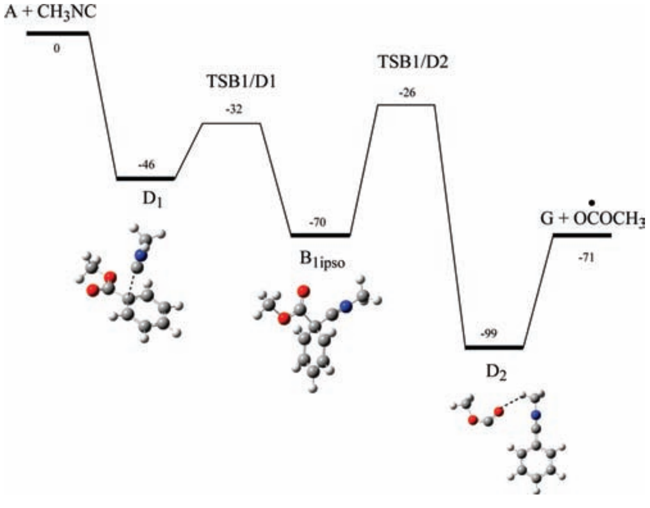

Figure 1. Computed 298 K enthalpy (kJ mol^{-1}) diagram associated with the loss of $^{\bullet}$OCOCH$_3$.

Hydrogen Atom Loss. This reaction represents the minor dissociation process of the **A** + CH$_3$NC adducts. Using methyl benzoate-d_5 (ring deuterated), it clearly appears that the eliminated hydrogen atom comes specifically from the benzene ring. The simplest hypothesis which may account for the formation of the *m*/*z* 176 ions is to assume a direct loss of the angular hydrogen situated on the ring of the three covalent structures $\mathbf{B_{1ortho}}$, $\mathbf{B_{1meta}}$, and $\mathbf{B_{1para}}$. These fragmentations would give rise to the corresponding methoxycarbonyl *N*-methyl benzonitrilium cations $\mathbf{E_{1ortho}}$, $\mathbf{E_{1meta}}$, and $\mathbf{E_{1para}}$, which correspond indeed to fragmentation products more stable than the reactants by 10−30 kJ mol^{-1} (Scheme 3).

In the case of the ortho structure, however, the formation of a cyclized *m*/*z* 176 ion $\mathbf{E_{2ortho}}$ (Schemes 3 and 4) may be expected if the closure of the five-membered ring brings an overstabilization. Computation indicates that it is not the case: the cyclized structure $\mathbf{E_{2ortho}}$ is less stable than its open isomer $\mathbf{E_{1ortho}}$ by 19 kJ mol^{-1} (Table 1, Scheme 4). In fact, several conformations are expected for ions $\mathbf{E_{1ortho}}$ and $\mathbf{E_{2ortho}}$. The investigated possibilities are summarized in Scheme 4 (note that structure $\mathbf{E_{1ortho'''}}$ has not been identified, all attempts leading to conformer $\mathbf{E_{1ortho''}}$).

It appears that structures $\mathbf{E_{1ortho}}$ and $\mathbf{E_{2ortho}}$ are the most stable in their categories and that cyclized forms are always less stable than their open analogues by ca. 20 kJ mol^{-1}. Cyclic structures where the methyl of the imino group is opposed to the oxygen atom of the furan ring are destabilized by an additional amount of 20 kJ mol^{-1} (Table 1, Scheme 4).

SCHEME 3

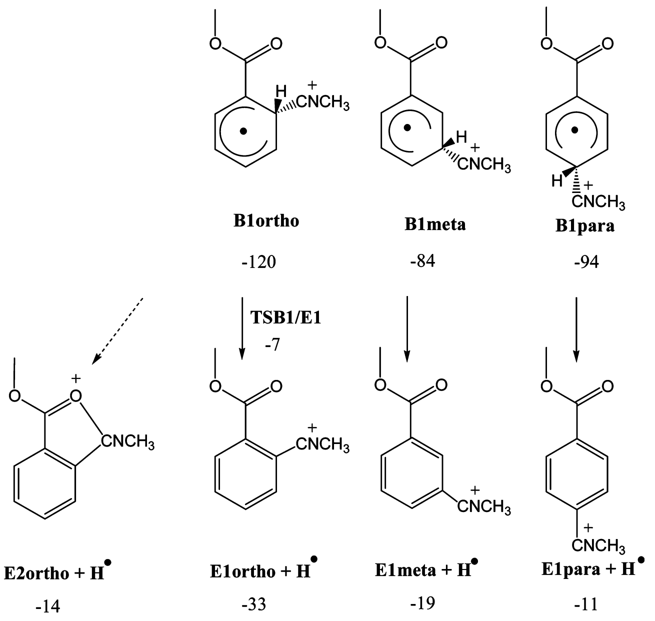

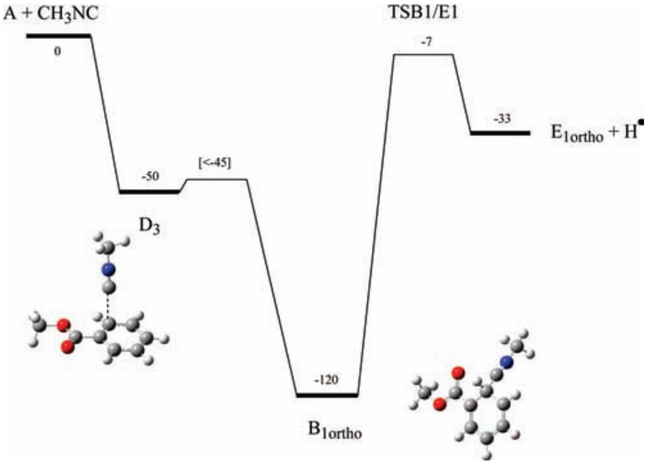

Figure 2. Computed 298 K enthalpy (kJ mol^{-1}) diagram associated with the loss of $^{\bullet}H$.

Considering the exothermicity as a criterion of reaction feasibility, the four possibilities depicted in Scheme 3 may be retained. However, the occurrence of critical energy barriers during the addition−elimination steps should be taken into account. We thus investigated the overall reaction leading to the most stable products **A** + $CH_3NC \rightarrow$ $\mathbf{E_{1ortho}}$ + $H^{\bullet}$. Results are illustrated in Figure 2.

During the approach of the reactants **A** and CH_3NC, a first ion−neutral complex, **D3**, is produced. This structure, characterized by a C_{ortho}.. .$CNCH_3$ distance of 2.40 Å, is situated 50 kJ mol^{-1} below **A** + CH_3NC. A progressive shortening of this distance leads to a very slight increase (less than 5 kJ mol^{-1}) followed by a significant decrease of the potential energy until attaining the structure $\mathbf{B_{1ortho}}$. The step **D3** → $\mathbf{B_{1ortho}}$ is comparable to the **D1** → $\mathbf{B_{1ipso}}$ process depicted in the part devoted to the $OCOCH_3$ loss. The lack of a noticeable critical energy associated with the reaction **D3** → $\mathbf{B_{1ortho}}$ is probably related to the very large energy gain accompanying the C−C covalent bond formation. Starting from $\mathbf{B_{1ortho}}$, the C(ortho)−H bond elongation is associated with a considerable increase of the total energy which passes through a maximum situated more than 110 kJ mol^{-1} above $\mathbf{B_{1ortho}}$ for a C.. .H distance of 1.803 Å. This was expected since the complete planarity of the ring and the $CNCH_3$ moiety cannot be attained before a large increase of the C−H distance. The transition structure **TSB1/E1** has been characterized; its 298 K enthalpy is situated only 7 kJ mol^{-1} below the reactants **A** + CH_3NC. After passing this transition structure, the C.. .H elongation is followed by a stabilization of the system when attaining the fragments $\mathbf{E_{1ortho}}$ + $H^{\bullet}$. No complex involving $\mathbf{E_{1ortho}}$ and $H^{\bullet}$ has been identified. It consequently appears that a reverse reaction enthalpy of 26 kJ mol^{-1} is associated with the reaction $\mathbf{B_{1ortho}} \rightarrow \mathbf{E_{1ortho}}$ + $H^{\bullet}$. If a similar effect is associated with the hydrogen atom loss from structures $\mathbf{E_{1meta}}$ and $\mathbf{E_{1para}}$, the corresponding transition structures are predicted to be higher in enthalpy than **A** + CH_3NC by 7 and 15 kJ mol^{-1}, respectively. Participation of these two structures in the hydrogen loss process is thus probably limited, and the most reasonable path for the hydrogen atom loss is consequently that leading to $\mathbf{E_{1ortho}}$ (Figure 2).

The CA spectrum of *m*/*z* 176 ions has been tentatively examined. In spite of the very low intensity of the parent ion signal, peaks at *m*/*z* 135 and 117 are noticeable. They may be attributed to losses of isonitrile and methoxyacyl radical, respectively, and thus corroborate the assignment to structures in which these two groups had preserved their identities such as $\mathbf{E_{1ortho}}$, $\mathbf{E_{1meta}}$, or $\mathbf{E_{1para}}$ (Scheme 3).

SCHEME 4

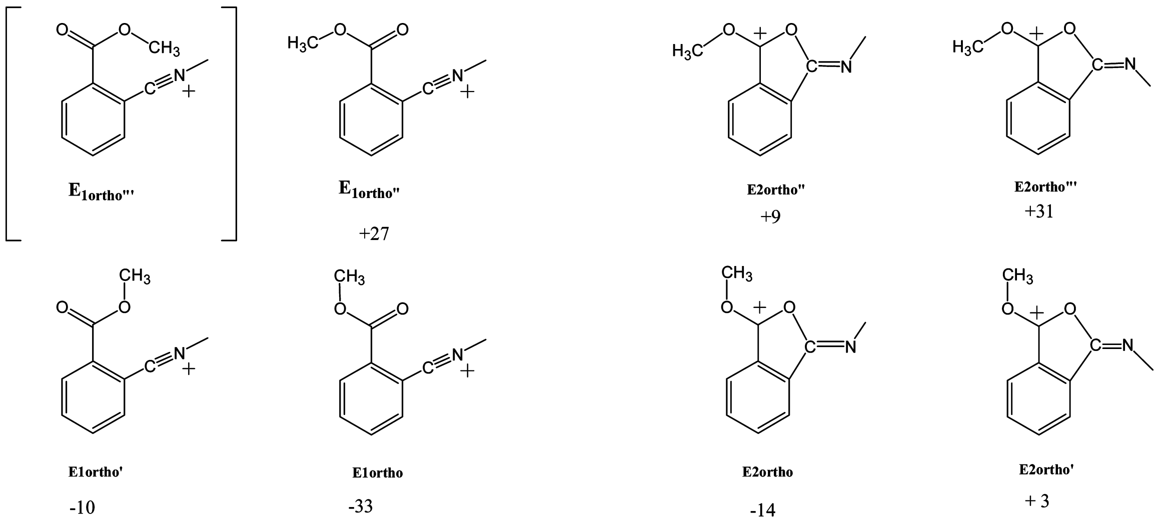

SCHEME 5

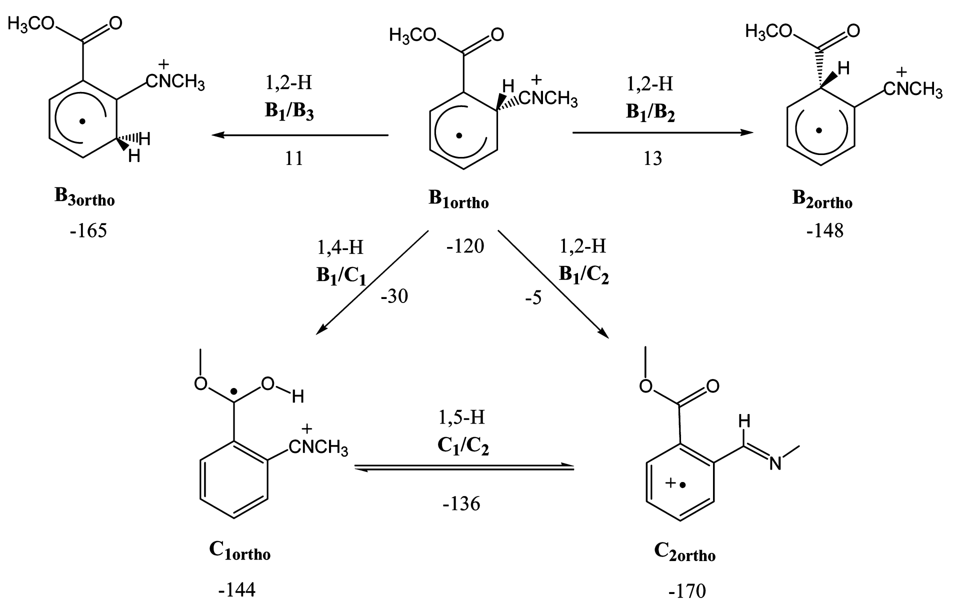

SCHEME 6

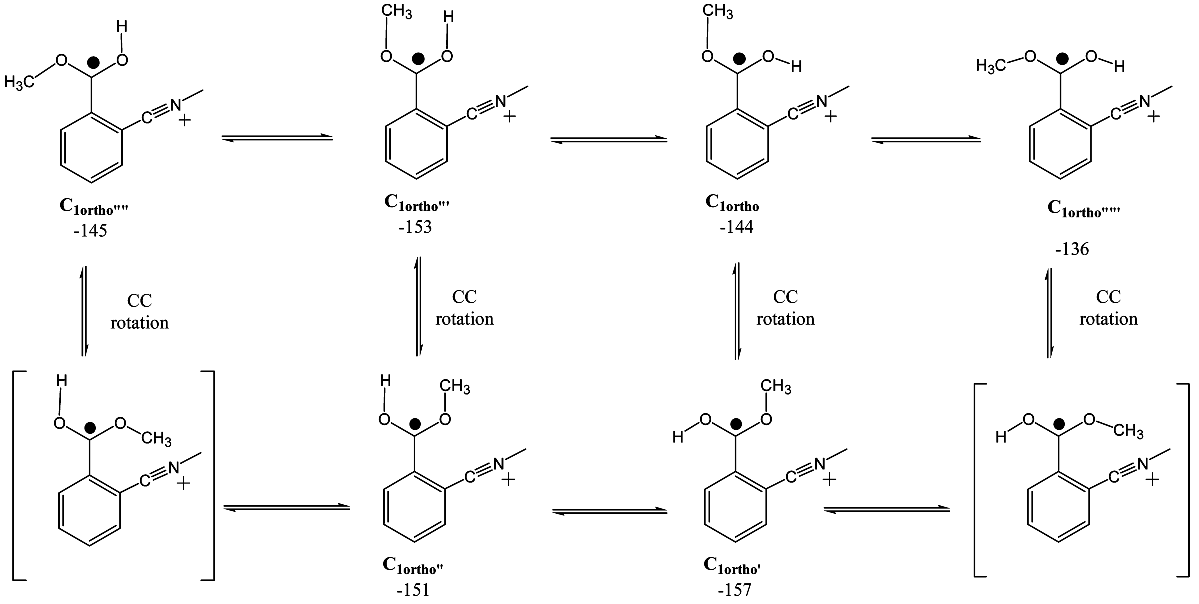

Methyl Group Loss. Reaction between d_3-methyl deuterated benzoate and methyl isonitrile shows that the methyl loss occurs exclusively from the ester function, not the isonitrile moiety. Direct methyl loss from an ionized carbomethoxy group is rare since a R−COO$^+$ cationic species is not thermochemically stable. Consequently, the formation of m/z 162 ions should be associated with some rearrangement of the initial adducts $\mathbf{B_{1ipso}}$, $\mathbf{B_{1ortho}}$, $\mathbf{B_{1meta}}$, $\mathbf{B_{1para}}$, or $\mathbf{B_{oxo}}$ (see Scheme 1).

Starting from the most stable structure, namely, $\mathbf{B_{1ortho}}$, two major routes were investigated where the angular hydrogen atom brought by the sp^3 carbon of the ring participates in a 1,4- or a 1,2-migration (Scheme 5). The 1,2-H migration process, leading to structure $\mathbf{C_{2ortho}}$, needs the largest critical energy. However, it is theoretically allowed since the transition structure $\mathbf{TSB_1/C_2}$ is more stable than **A** + CH_3NC by 5 kJ mol^{-1}. The reaction involving the 1,4-H migration, $\mathbf{B_{1ortho}} \rightarrow \mathbf{C_{1ortho}}$, is energetically easier: the transition structure $\mathbf{TSB_1/C_1}$ is 25 kJ mol^{-1} lower in energy than $\mathbf{TSB_1/C_2}$. It is difficult to discuss the competition between the two reactions $\mathbf{B_{1ortho}} \rightarrow \mathbf{C_{1ortho}}$ and $\mathbf{B_{1ortho}} \rightarrow \mathbf{C_{2ortho}}$ only in first law terms because both processes are rearrangements for which frequency factors (entropies of reaction) are certainly different. Particularly, the 1,4-H migration favored by its low critical energy is also probably disfavored by a low frequency factor. Whatever the rate of formation of $\mathbf{C_{1ortho}}$ and $\mathbf{C_{2ortho}}$, the coexistence of both structures is favored by their facile interconversion. Indeed, the $\mathbf{C_{1ortho}} \rightarrow \mathbf{C_{2ortho}}$ reaction is a 1,5-H migration associated with a very low critical energy: the transition structure $\mathbf{TSC_1/C_2}$ is 136 kJ mol^{-1} more stable than the reactants and less than 10 kJ mol^{-1} above $\mathbf{C_{1ortho}}$. We can thus consider that a mixture of $\mathbf{C_{1ortho}}$ and $\mathbf{C_{2ortho}}$ is readily produced from reaction between **A** and CH_3NC.

Note that other isomerization processes are possible from $\mathbf{B_{1ortho}}$. This is, for example, the case of 1,2-H migrations inside the benzenic moiety which may be at the origin of a possible ring walk of the angular hydrogen (Scheme 5). The two first structures attainable by these reactions are $\mathbf{B_{2ortho}}$ and $\mathbf{B_{3ortho}}$, which present stabilities situated between that of $\mathbf{B_{1ortho}}$ and $\mathbf{C_{2ortho}}$. However, the critical energies of the 1,2-H migrations connecting $\mathbf{B_{1ortho}}$ to these two species are too high to allow a significant competition with the formations of $\mathbf{C_{1ortho}}$ or $\mathbf{C_{2ortho}}$.

SCHEME 7

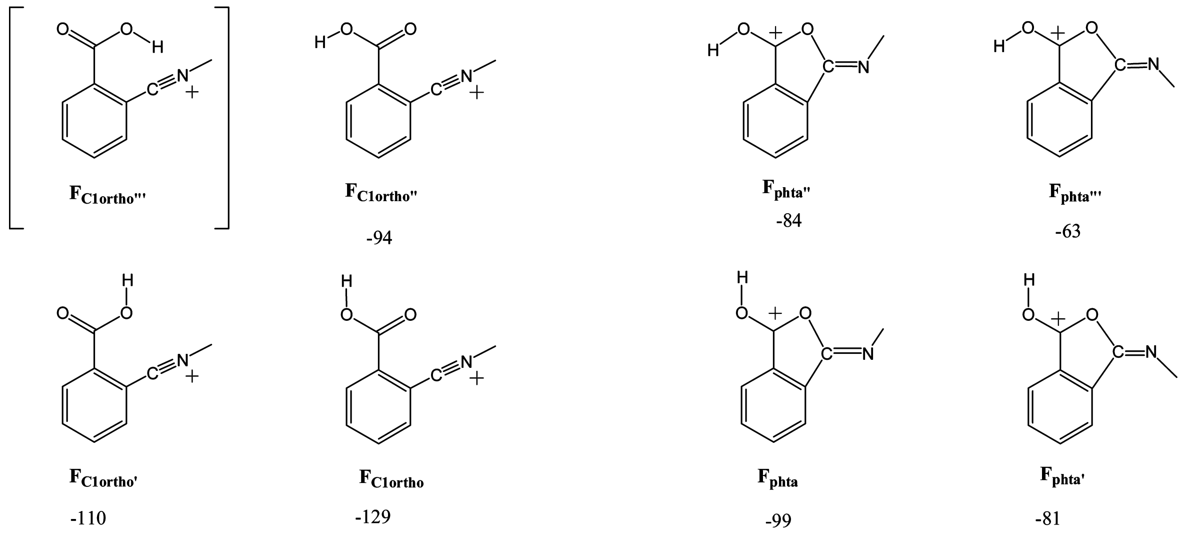

Accordingly, the transition state 298 K enthalpies of $\mathbf{B_{1ortho}} \rightarrow \mathbf{B_{2ortho}}$ ($\mathbf{TSB_1/B_2}$) and $\mathbf{B_{1ortho}} \rightarrow \mathbf{B_{3ortho}}$ ($\mathbf{TSB_1/B_3}$) are equal to 13 and 11 kJ mol^{-1}, respectively.

Pathways to the methyl radical elimination were further explored starting from $\mathbf{C_{1ortho}}$ and $\mathbf{C_{2ortho}}$ structures. Considering first the isomeric form $\mathbf{C_{1ortho}}$, rotations around the C−OH and C−OCH_3 bonds and of the $C(OH)(OCH_3)$ moiety with respect to the aromatic ring (C−C rotation) may a priori interconnect eight conformers (Scheme 6). In fact, only six structures (denoted $\mathbf{C_{1ortho..}}$ in Scheme 6) have been found to correspond to local minima.

The energies of the most stable rotamers are reported in Table 1, and their 298 K enthalpies relative to the reactants **A** + CH_3NC are indicated below the corresponding structure in Scheme 6. Each of these structures is able to expel the methyl radical of the methoxy group giving either *N*-methylated 2-cyanobenzoic acid, $\mathbf{F_{C1ortho}}$, or a protonated phthalate derivative, $\mathbf{F_{phta}}$, if a cyclization assists the methyl elimination. The possible candidates are gathered in Scheme 7 where are also noted the computed 298 K enthalpies of the products *m*/*z* 116 + $^{\bullet}CH_3$ relative to **A** + CH_3NC.

Several observations can be made concerning the computed *m*/*z* 162 ion structure which parallels results discussed for the homologue ions *m*/*z* 176 (Scheme 3). First, all guesses for the geometry of $\mathbf{F_{C1ortho'''}}$ converge on its CC rotamer $\mathbf{F_{C1ortho''}}$ (Scheme 7). Second, it is found again that the cyclized forms ($\mathbf{F_{phta}}$) are less stable than their open counterparts ($\mathbf{F_{C1ortho}}$). The cyclized forms $\mathbf{F_{phta''}}$ and $\mathbf{F_{phta}}$ are less stable than their open homologues $\mathbf{F_{C1ortho''}}$ and $\mathbf{F_{C1ortho}}$ by 10 and 30 kJ mol^{-1}, respectively. A similar result was observed for the open and cyclized ions **E** (Scheme 3); however, the energy difference was uniformly equal to 20 kJ/mol. The $C{=}NCH_3$ syn/anti conformers exhibit differences in energy close to 20 kJ mol^{-1}, a value comparable to what was observed for the ions $\mathbf{E_{2orthox}}$. Even though all the identified structures reported in Scheme 7 are possible candidates for the *m*/*z* 162 ions, we investigated in detail only the lowest energy routes leading to the most stable structures $\mathbf{F_{C1ortho}}$ and its closely related rotamer $\mathbf{F_{C1ortho''}}$. Rotational barriers $\mathbf{C_{1ortho}} \rightarrow \mathbf{C_{1ortho'}}$ and $\mathbf{C_{1ortho'}} \rightarrow \mathbf{C_{1ortho''}}$ have been estimated by considering the intermediate structure where the dihedral angle is frozen to 90°. The corresponding energies are sufficiently low with respect to the reactants **A** + CH_3NC so that it is not useful to precisely locate the transition structures for these processes. The results are summarized in Scheme 8.

SCHEME 8

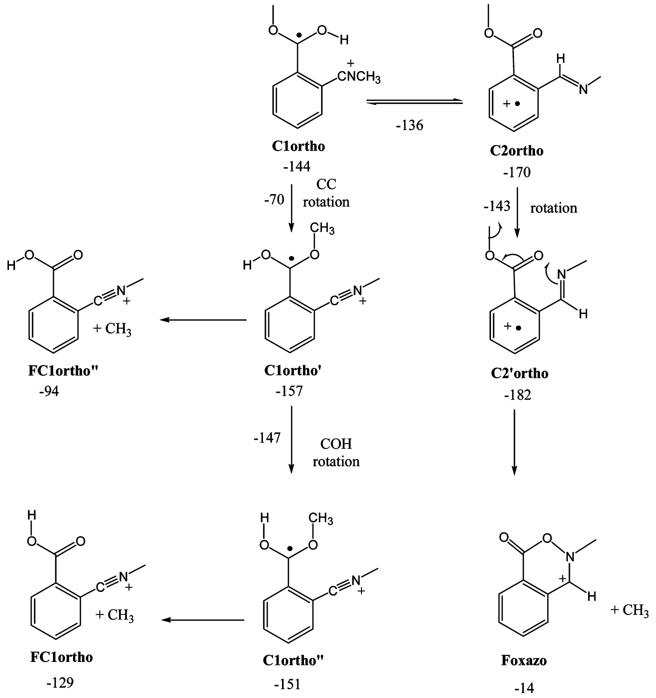

Considering now structure $\mathbf{C_{2ortho}}$ as a starting point, a direct methyl loss is not possible because it would produce an unstable $RCOO^+$ ion. A less energy-demanding process would be to form a cyclized ion such as the oxazinone derivative $\mathbf{F_{oxazo}}$ (Scheme 8). A prerequisite for this formation is a rotation of the $CH{=}NCH_3$ group, $\mathbf{C_{2ortho}} \rightarrow \mathbf{C_{2'ortho}}$. This rotation needs less than 30 kJ mol^{-1} and is thus free to occur. The second step, the cyclization-assisted methyl elimination, needs at least the endothermicity of the reaction $\mathbf{C_{2'ortho}} \rightarrow \mathbf{F_{oxazo}}$ + $^{\bullet}CH_3$. As indicated in Table 1 and in Scheme 8, this latter set of products is situated only 14 kJ mol^{-1} below **A** + CH_3NC. Consequently, the two ionic products $\mathbf{F_{C1ortho''}}$ (or $\mathbf{F_{C1ortho'}}$) and $\mathbf{F_{oxazo}}$ differ by ca. 80 kJ mol^{-1}, and it is thus probable that the formation of the former species would be favored over the latter. Figure 3 summarizes the various reaction path examined using $\mathbf{B_{1ortho}}$ as precursor.

Another possible explanation for the *m*/*z* 162 ion formation is that the CH_3 loss occurs from structure $\mathbf{B_{1oxo}}$ (Scheme 9).

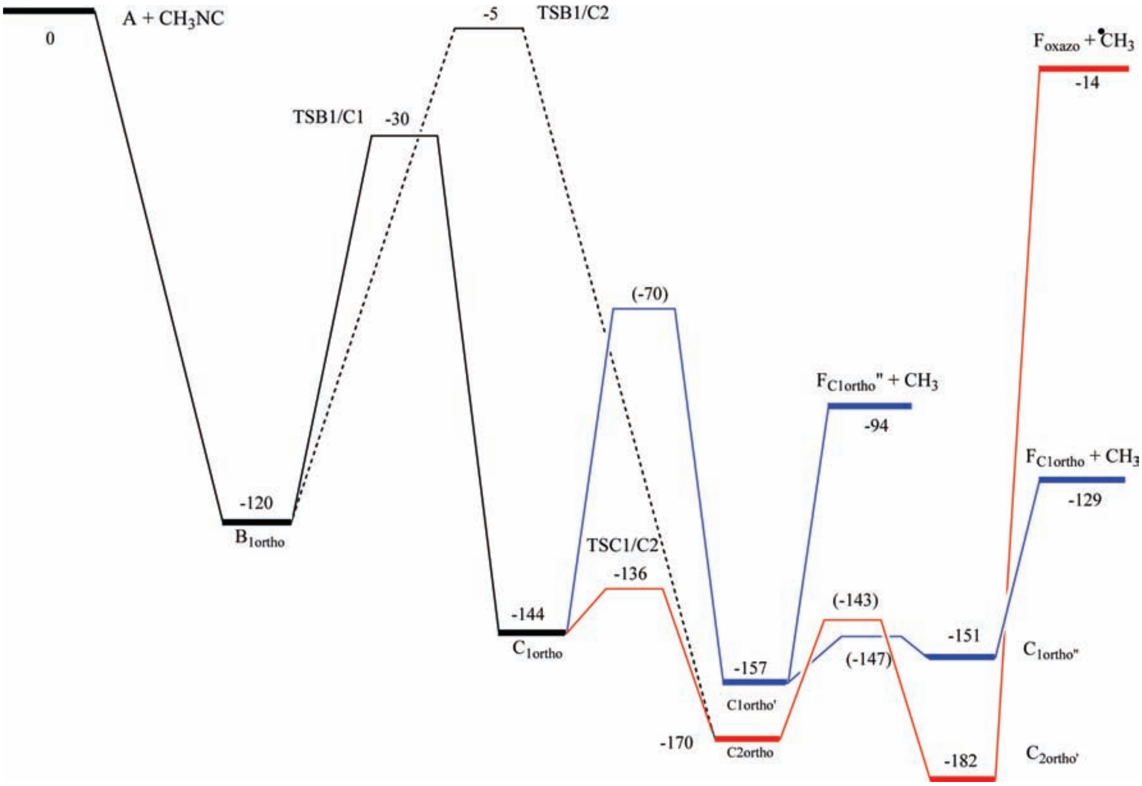

Figure 3. Computed 298 K enthalpy (kJ mol^{-1}) diagram associated with the various isomerization/dissociation processes proposed to explain the $^{\bullet}CH_3$ loss from the ortho adduct $\mathbf{B_{1ortho}}$.

SCHEME 9

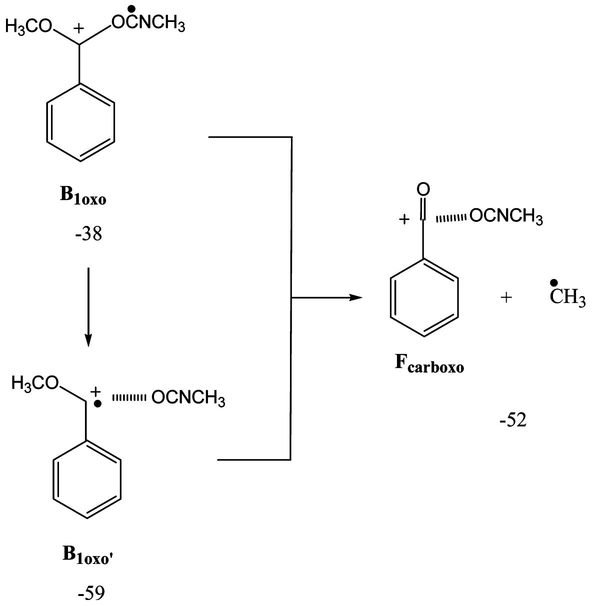

The expected ionic product, $\mathbf{F_{carboxo}}$, is in fact an ion neutral complex between benzoyl cation and CH_3NCO. The products $\mathbf{F_{carboxo}} + {}^{\bullet}CH_3$ are situated 52 kJ mol^{-1} below $\mathbf{A}$ + CH_3NC and are consequently possible candidates. However, here again, it is necessary to examine the total energy change associated with the reaction $\mathbf{B_{1oxo}} \rightarrow \mathbf{F_{carboxo}} + {}^{\bullet}CH_3$. This process is not a "simple" bond cleavage since it involves two C−O bond elongations, one leading to the methyl elimination and the second being responsible for the ion neutral interaction (2.758 Å, Figure 2). Direct elongation of the CH_3−O bond in the $\mathbf{B_{1oxo}}$ structure is associated with a very sharp energy change; an increase of 0.5 Å leads to an increase of more than 100 kJ mol^{-1} in total energy. Considering the fact that $\mathbf{B_{1oxo}}$ is only 38 kJ mol^{-1} below the reactants $\mathbf{A}$ + CH_3NC, it seems unlikely that this reaction may explain the observation of the *m/z* 162 ion.

A second possibility was explored where the C.. .$OCNCH_3$ bond was first elongated in the $\mathbf{B_{1oxo}}$ structure. Interestingly enough, this route leads to a second local minimum, $\mathbf{B_{1oxo'}}$, which corresponds to a complex between a CH_3NCO neutral and a $[C_6H_5COCH_3]^{\bullet+}$ radical cation. This latter is in fact an ionized carbene, as attested by the Mulliken population analysis. The stability of this $[C_6H_5C^{\bullet+}OCH_3]$ species is not surprising since it is known that both a phenyl ring and a methoxy group stabilize radical and charged sites.[32] Complex $\mathbf{B_{1oxo'}}$ is more stable than $\mathbf{B_{1oxo}}$ by ~20 kJ·mol^{-1}. However, starting from $\mathbf{B_{1oxo'}}$, the CH_3−O bond elongation inside the ionized carbene moiety is significantly energy consuming, thus rendering this reaction hardly competitive with the "$\mathbf{C_{1ortho}}$" pathway (Figure 3).

Conclusion

Two aromatic substitution reactions involving ionized methyl benzoate and neutral methyl isocyanide were studied theoretically. In the first, major, reaction, methyl isocyanide displaces the methoxyacyl radical to give *N*-methylated benzonitrile cation. The second, minor, substitution process is associated with a hydrogen atom loss leading probably to *N*-methylated benzonitrile substituted at the ortho position by a carboxylic group ($\mathbf{E_{1ortho}}$ structure, Scheme 4). It is shown that both reactions are multistep processes involving ion−neutral approach complexes ($\mathbf{D_1}$, Figure 1, and $\mathbf{D_3}$, Figure 2) and σ-complexes intermediates ($\mathbf{B_{1ipso}}$, Figure 1, and $\mathbf{B_{1ortho'}}$, Figure 2). The latter complexes are lying in deep energy wells situated 70 and 120 kJ/mol, respectively, below the reactants, ionized methyl benzoate and methyl isocyanide. The rate-determining step of both elimination reactions is the passage from the covalent intermediate to the exit channel. The abundances of the products seem to be correlated with the height of the corresponding energy barrier since the *m/z* 118 and 176 ions abundances are equal to 100% and 2% while the 298 K enthalpies are −26 and −7 kJ/mol, respectively. A third reaction, competitive with the two former nucleophilic aromatic substitutions, involves multiple hydrogen migrations before the loss of the methyl radical from the original methoxy carbonyl moiety of ionized methyl benzoate (Figure 3). It is noteworthy that the σ-complex, $\mathbf{B_{1ortho}}$, is at the origin of this rearrangement. A mixture of *m/z* 162 ion structures is probably produced, among which *N*-methylated cyano benzoic acids, $\mathbf{F_{C1orthox}}$ (Schemes 7 and 8), are the best candidates.

Acknowledgment. We thank the Fonds National de la Recherche Scientifique (FNRS) for financial support in the acquisition of the large-scale tandem mass spectrometer. P.G. also thanks the FNRS for continuing support.

References and Notes

(1) Terrier, F. *Chem. Rev.* **1982**, *82*, 77.

(2) Buncel, E.; Dust, J. M.; Terrier, F. *Chem. Rev.* **1995**, *95*, 2261.

(3) Wheland, G. W. *J. Am. Chem. Soc.* **1942**, *64*, 900.

(4) Chiavarino, B.; Crestoni, M. E.; Fornarini, S.; Lanucara, F.; Lemaire, J.; Maitre, P. *Angew. Chem., Int. Ed.* **2007**, *46*, 1995.

(5) Lorenz, U.; Solca, N.; Dopfer, O. *Chem. Phys. Lett.* **2005**, *406*, 321.

(6) Hasegawa, H.; Mizuze, K.; Hachiya, M.; Matsuda, Y.; Mikami, N.; Fujii, A. *Angew. Chem., Int. Ed.* **2008**, *47*, 6008.

(7) Danikiewicz, W.; Bienkowski, T.; Kozlowska, D.; Zimnicka, M. *J. Am. Soc. Mass Spectrom.* **2007**, *18*, 1351, and references cited therein.

(8) Maeyama, T.; Mikami, N. *J. Am. Chem. Soc.* **1988**, *110*, 7238.

(9) Maeyama, T.; Mikami, N. *J. Phys. Chem.* **1990**, *94*, 6973.

(10) Maeyama, T.; Mikami, N. *J. Phys. Chem.* **1991**, *95*, 7197.

(11) Tachikawa, H. *J. Phys. Chem. A* **2006**, *110*, 153.

(12) Thölmann, D.; Grützmacher, H.-Fr. *Chem. Phys. Lett.* **1989**, *163*, 225.

(13) Thölmann, D.; Grützmacher, H.-Fr. *Org. Mass Spectrom.* **1989**, *24*, 439.

(14) Thölmann, D.; Grützmacher, H.-Fr. *J. Am. Chem. Soc.* **1991**, *113*, 3281.

(15) Flammang, R.; De Winter, J.; Gerbaux, P. *Eur. J. Mass Spectrom.* **2008**, *14*, 299.

(16) Dechamps, N.; Flammang, R.; Boulvin, M.; Gerbaux, P. *Eur. J. Mass Spectrom.* **2007**, *13*, 385.

(17) Dechamps, N.; Flammang, R.; Boulvin, M.; Lamote, L.; Gerbaux, P.; Nam, P. C.; Nguyen, M. T. *Int. J. Mass Spectrom.* **2006**, *249/250*, 484.

(18) Dechamps, N.; Flammang, R.; Gerbaux, P.; Nam, P. C.; Nguyen, M. T. *Int. J. Mass Spectrom.* **2008**, *270*, 101.

(19) Hunter, E. P.; Lias, S. G. *Standard reference database no. 69. NIST Chemistry Webbook*; National Institute of Standards and Technology: Gaithersburg, MD, 2005; http//webbook.nist.gov/chemistry/.

(20) Dechamps, N.; Flammang, R.; Gerbaux, P.; Nam, P. C.; Nguyen, M. T. *Int. J. Mass Spectrom.* **2006**, *249*−*250*, 484.

(21) Dechamps, N.; Flammang, R.; Gerbaux, P.; Nam, P. C.; Nguyen, M. T. *J. Am. Chem. Soc. Mass Spectrom.* **2006**, *17*, 807.

(22) Huang, Y.; Peterman, S.; Tichy, S. E.; North, S. W.; Russell, D. H. *J. Phys. Chem. A* **2008**, *112*, 11590.

(23) Frisch, M. J.; Trucks, G. W.; Schlegel, H. B.; Scuseria, G. E.; Robb, M. A.; Cheeseman, J. R.; Montgomery, J. A.; Vreven, T., Jr.; Kudin, K. N.; Burant, J. C.; Millam, J. M.; Iyengar, S. S.; Tomasi, J.; Barone, V.; Mennucci, B.; Cossi, M.; Scalmani, G.; Rega, N.; Petersson, G. A.; Nakatsuji, H.; Hada, M.; Ehara, M.; Toyota, K.; Fukuda, R.; Hasegawa, J.; Ishida, M.; Nakajima, T.; Honda, Y.; Kitao, O.; Nakai, H.; Klene, M.; Li, X.; Knox, J. E.; Hratchian, H. P.; Cross, J. B.; Adamo, C.; Jaramillo, J.; Gomperts, R.; Stratmann, R. E.; Yazyev, O.; Austin, A. J.; Cammi, R.; Pomelli, C.; Ochterski, J. W.; Ayala, P. Y.; Morokuma, K.; Voth, G. A.; Salvador, P.; Dannenberg, J. J.; Zakrzewski, V. G.; Dapprich, S.; Daniels, A. D.; Strain, M. C.; Farkas, O.; Malick, D. K.; Rabuck, A. D.; Raghavachari, K.; Foresman, J. B.; Ortiz, J. V.; Cui, Q.; Baboul, G.; Clifford, S.; Cioslowski, J.; Stefanov, B. B.; Liu, G.; Liashenko, A.; Piskorz, P.; Komaromi, I.; Martin, R. L.; Fox, D. J.; Keith, T.; Al-Laham, M. A.; Peng, C. Y.; Nanayakkara, A.; Challacombe, M.; Gill, P. M. W.; Johnson, B.; Chen, W.; Wong, M. W.; Gonzalez, C.; Pople, J. A. *Gaussian 03*, revision B.04; Gaussian, Inc.: Pittsburgh, PA, 2003.

(24) Riley, K. E.; Op't Holt, B. T.; Merz, K. M., Jr. *J. Chem. Theory Comput.* **2007**, *3*, 407.

(25) Sousa, S. F.; Fernandes, P. A.; Ramos, M. J. *J. Phys. Chem. A* **2007**, *111*, 10439.

(26) Tirado-Rives, J.; Jorgensen, W. L. *J. Chem. Theory Comput.* **2008**, *4*, 297.

(27) Rao, L.; Ke, H.; Fu, G.; Xu, X.; Yan, Y. *J. Chem. Theory Comput.* **2009**, *5*, 86.

(28) Henry, D.; Parkinson, C. J.; Mayer, P. M.; Radom, L. *J. Phys. Chem. A* **2001**, *105*, 6750.

(29) Henry, D.; Sullivan, M. B.; Radom, L. *J. Chem. Phys.* **2003**, *118*, 4849.

(30) Menon, A. S.; Wood, G. P. F.; Moran, D. M.; Radom, L. *J. Phys. Chem. A* **2007**, *111*, 13638.

(31) Ruttink, P. J. A.; Burgers, P. C.; Fell, L. M.; Terlouw, J. K. *J. Phys. Chem. A* **1999**, *103*, 1426.

(32) Flammang, R.; Nguyen, M. T.; Gerbaux, P.; Bouchoux, G. *Int. J. Mass Spectrom.* **2000**, *202*, 8.

JP906942E